# Soliton management for a variable-coefficient modified Korteweg–de Vries equation

Zhi-Yuan Sun,[1] Yi-Tian Gao,[1,2,*] Ying Liu,[1] and Xin Yu[1]

[1]*Ministry-of-Education Key Laboratory of Fluid Mechanics and National Laboratory for Computational Fluid Dynamics, Beijing University of Aeronautics and Astronautics, Beijing 100191, China*

[2]*State Key Laboratory of Software Development Environment, Beijing University of Aeronautics and Astronautics, Beijing 100191, China*

(Received 8 June 2010; revised manuscript received 5 June 2011; published 5 August 2011)

The concept of soliton management has been explored in the Bose-Einstein condensate and optical fibers. In this paper, our purpose is to investigate whether a similar concept exists for a variable-coefficient modified Korteweg–de Vries equation, which arises in the interfacial waves in two-layer liquid and Alfvén waves in a collisionless plasma. Through the Painlevé test, a generalized integrable form of such an equation has been constructed under the Painlevé constraints of the variable coefficients based on the symbolic computation. By virtue of the Ablowitz-Kaup-Newell-Segur system, a Lax pair with time-dependent nonisospectral flow of the integrable form has been established under the Lax constraints which appear to be more rigid than the Painlevé ones. Under such Lax constraints, multisoliton solutions for the completely integrable variable-coefficient modified Korteweg–de Vries equation have been derived via the Hirota bilinear method. Moreover, results show that the solitons and breathers with desired amplitude and width can be derived via the different choices of the variable coefficients.

DOI: 10.1103/PhysRevE.84.026606 PACS number(s): 05.45.Yv, 47.35.Fg, 02.30.Jr

## I. INTRODUCTION

Since the first introduction of the soliton concept [1], the classical nonlinear evolution equations (NLEEs) which support soliton solutions, such as the modified Korteweg–de Vries (mKdV) and nonlinear Schrödinger (NLS) equations, have been proposed to describe a variety of physical phenomena in the fields of hydrodynamics, ocean dynamics, plasma physics, Bose-Einstein condensate (BEC), and optical fibers [2–8]. Meanwhile, different methods have been developed to address those NLEEs for deriving their soliton solutions [2].

Based on the significance of the nonlinear mechanisms in different physical fields, Ref. [3] has stated that it is necessary to investigate the soliton dynamics to provide theoretical tools for supporting the relevant physical phenomena and experiments. In such case, the concept of soliton management which is claimed to be of some physical applications [4], such as the Feshbach resonance and dispersion management in the BEC and dispersion and nonlinearity management in the optical fibers, has been explored [3–5]. For example, Ref. [4] has presented the dispersion and nonlinearity management for the femtosecond optical solitons and studied the optimal amplification of solitons through dispersion wells and barriers. Reference [5] has proposed a scheme to control the dynamics of the localized states in a one-dimensional BEC, periodically flipping the sign of the scattering length via the Feshbach resonance, which is named the Feshbach-resonance management.

As one technique of the soliton management, the dispersion management has received attention for improving the operation characteristics (i.e., stability and bit rates) of the solitons in the optical fibers [6] or reducing certain negative effects (i.e., radiation, jitters, resonant four-wave mixing, and the Gordon-Haus effect) [7]. Reference [8] has employed the dispersion management to study the interaction features of the optical solitons, such as the soliton-width compression, soliton-energy control, and soliton-pulse amplification. However, such a technique is mainly focused on the BEC and optical fiber systems described by the NLS-typed models [4–8]. With this consideration, Ref. [6] extends the concept of dispersion management to the internal waves in stratified fluids governed by a KdV system with a periodic modulation of the dispersion coefficient, and presents the existence of the stable solitary-wave solutions in the region defined by the average dispersion and initial momentum [6]. Therefore, it is possible to extend the concept of soliton management to other NLEEs with physical backgrounds, such as the mKdV equation which can describe the interfacial waves in the two-layer liquid with gradually varying depth [9].

Generally speaking, the soliton management can be realized with the four basic parameters featuring the dynamics of a soliton: the amplitude (or width), frequency (or velocity), phase, and time position [3]. It is known that the classical solitons behave like particles during the propagation and preserve their shapes and velocities with only phase shift after their interactions [2]. As the extension of the classical soliton concept, Ref. [10] reports that the soliton can propagate with time-invariant amplitudes but changeable velocities as time evolution in a linearly inhomogeneous plasma, which is described by the NLS equation with a linear external potential. At the same time, the analytical soliton solutions are also derived from the KdV equation with varying nonlinearity and dispersion [11]. We notice that the soliton management for the NLS and KdV models can be achieved by the control of the soliton amplitudes and velocities. Consequently, in Ref. [12], the soliton with time-variant amplitude and velocity is suggested to be named the nonautonomous soliton, which is one type of solution for the nonautonomous system with time- or space-dependent dispersion and nonlinearity [12]. Moreover, in those nonautonomous systems, the constant spectral parameter in the inverse scattering method should be extended to the nonisospectral time-dependent function [12,13].

*gaoyt@public.bta.net.cn

 

In this paper, from the viewpoint of manipulating the soliton dynamics, we will investigate the soliton management for a variable-coefficient mKdV equation,

$$u_t + a(x,t)\,u^2\,u_x + b(x,t)\,u_{xxx} + c(x,t)\,u_x + d(x,t)\,u = 0, \tag{1}$$

where $u(x,t)$ is a function of the scaled space $x$ and time $t$, $a(x,t)$, $b(x,t)$, $c(x,t)$, and $d(x,t)$ account for the cubic nonlinear, dispersion, nonuniformity term, and line-damping coefficients, respectively. Equation (1) is not completely integrable unless the variable coefficients satisfy certain constraint conditions, such as the standard mKdV equation describing the interfacial waves in two-layer liquid [9], propagation of an elastic quasiplane wave in a lattice [14], and Alfvén waves in a collisionless plasma [15], cylindrical mKdV equation with physical interest [16], and the following integrable variable-coefficient mKdV equation [16–22],

$$\begin{aligned} u_t =\ & K_0(t)\,(u_{xxx} - 6\,u^2\,u_x) + 4\,K_1(t)\,u_x \\ & - h(t)\,(u + x\,u_x) = 0, \end{aligned} \tag{2}$$

with $a(x,t) = 6\,K_0(t)$, $b(x,t) = -K_0(t)$, $c(x,t) = x\,h(t) - 4\,K_1(t)$, $d(x,t) = h(t)$ in Eq. (1). Integrable properties of Eq. (2) have been investigated from the different points of view in the previous attempts [16–22]: Ref. [16] has presented existence of the infinite conserved quantities; the solvability via the inverse scattering method and Lax pair representation related to the nonisospectral problem have been investigated in Ref. [17]; symmetries and Hamiltonian structures have also been constructed [18]; some explicit expressions of the solitonlike solutions have been derived through different types of methods, such as the symmetry reduction [19], the so-called Ricatti equation expansion method [20], and the variable-coefficient extended mapping method [21]. However, the soliton management for Eq. (2), namely, the control of the soliton amplitude and velocity, has not been explored to our knowledge, and the graphic illustration of the soliton propagations and their interactions could also be interesting to some extent. Moreover, although some special integrable cases of Eq. (1) have been studied from the viewpoint of integrable properties, it seems that further study on Eq. (1) is of certain value, especially in the sense of the Painlevé and complete integrability.

Therefore, in this paper, in order to discuss the dynamics of the solitons governed by Eq. (1), firstly it will be necessary to investigate the integrability of Eq. (1) in the Painlevé sense based on the Weiss-Talor-Carnevale (WTC) method [23] with the simplified Kruskal ansatz [24], and a generalized integrable form of Eq. (1) will be constructed when the variable coefficients satisfy certain constraints (the Painlevé constraints). Then under more rigid constraints (the Lax constraints), we will seek a nonisospectral Lax pair representation by virtue of the Ablowitz-Kaup-Newell-Segur (AKNS) system [25], which will be able to ensure the complete integrability of such integrable form for Eq. (1). Secondly, we will construct the multisoliton and breather solutions for such a completely integrable case by employing the Hirota bilinear method [26]. Furthermore, based on the explicit expressions of the solitons, we will discuss the effects of the nonuniformity term $c(x,t)$ on the soliton amplitude and velocity, and present the graphic illustration of the soliton interactions and breather propagations. In addition, numerical simulation will be performed to show the soliton dynamics with the Lax constraint finitely perturbed. Finally, we will present our conclusions.

## II. PAINLEVÉ ANALYSIS AND LAX PAIR

In order to determine the constraint conditions for Eq. (1) in the sense of the Painlevé integrability, we resort to the WTC method with the simplified Kruskal ansatz, which is an effective way to study the integrability of the partial differential equation (PDE) [23,24].

### A. Painlevé analysis

In order to simplify the calculations, we choose the simplified Kruskal ansatz with the noncharacteristic singularity manifold $\varphi(x,t)$ written as [24]

$$\varphi(x,t) = x + \phi(t), \tag{3}$$

and the solution $u(x,t)$ of Eq. (1) can be expressed in terms of the Laurent series,

$$u(x,t) = [x + \phi(t)]^{-\alpha} \sum_{j=0}^{\infty} u_j(t)\,[x + \phi(t)]^j, \tag{4}$$

where $u_j(t)$ and $\phi(t)$ are the arbitrary analytic functions with variable $t$ in the neighborhood of a noncharacteristic movable singularity manifold defined by $\varphi(x,t) = 0$, and $\alpha$ is a positive integer to be determined.

Variable coefficients $a(x,t)$, $b(x,t)$, $c(x,t)$, and $d(x,t)$ can be also expanded on the same singularity manifold as [27]

$$a(x,t) = \sum_{i=0}^{\infty} a_i(t)\,[x + \phi(t)]^i, \tag{5a}$$

$$b(x,t) = \sum_{i=0}^{\infty} b_i(t)\,[x + \phi(t)]^i, \tag{5b}$$

$$c(x,t) = \sum_{i=0}^{\infty} c_i(t)\,[x + \phi(t)]^i, \tag{5c}$$

$$d(x,t) = \sum_{i=0}^{\infty} d_i(t)\,[x + \phi(t)]^i, \tag{5d}$$

with

$$a_i(t) = \frac{1}{i!}\,\frac{\partial^i a(x,t)}{\partial x^i}\bigg|_{x=-\phi(t)}, \tag{6}$$

and $b_i(t)$, $c_i(t)$, $d_i(t)$ are similar to the expression of $a_i(t)$.

Substituting Expansions (5) into Eq. (1), via the balance between the dominant terms, we can derive $\alpha = 1$ and $a_0(t)\,u_0(t)^2 + 6\,b_0(t) = 0$. Without loss of generality, we choose $a(x,t)$ and $b(x,t)$ to be independent of $x$, that is, $a(x,t) = a_0(t) = a(t)$ and $b(x,t) = b_0(t) = b(t)$ in the following Painlevé test due to the complexity procedure.

By virtue of the symbolic computation [28,29], Resonances $-1$, 3, and 4 are found, where $j = -1$ corresponds to the arbitrariness of the singular manifold $\varphi(x,t)$. Resonances

$j = 3$ and 4 are verified if the following conditions on the variable coefficients are satisfied:

$$j = 3, \quad -2\,c_1(t) + 2\,d_0(t) - \frac{a'(t)}{a(t)} + \frac{b'(t)}{b(t)} = 0, \tag{7a}$$

$$j = 4, \quad c_2(t) - d_1(t) = 0, \tag{7b}$$

with the assumption that $c_2(t) = d_1(t) = 0$, which leads $d(x,t)$ to be space independent from the definition of $d_1(t) = \partial d(x,t)/\partial x|_{x=-\phi(t)}$. Hence, we have $d_1(t) = d_2(t) = \cdots = 0$ and $c_2(t) = c_3(t) = \cdots = 0$. The compatibility condition at $j = 4$ is satisfied automatically, and Eq. (7a) at $j = 3$ is one of the constraints on the variable coefficients which ensures that Eq. (1) can pass the Painlevé test.

Summarizing, we have the following:

*Proposition 2.1.* Equation (1) passes the Painlevé test if the following relations on the variable coefficients are verified,

$$\begin{aligned} &a(x,t) = a(t), \quad b(x,t) = b(t), \\ &c(x,t) = c_0(t) + x\,c_1(t), \quad d(x,t) = d_0(t) = d(t), \end{aligned} \tag{8}$$

where $a(t)$, $b(t)$, $c_1(t)$, and $d(t)$ satisfy constraint (7a), and $c_0(t)$ is the arbitrary function.

Therefore, we conclude that a generalized integrable form of Eq. (1) should have the following form:

$$\begin{aligned} &u_t + a(t)\,u^2\,u_x + b(t)\,u_{xxx} \\ &\quad + [c_0(t) + x\,c_1(t)]\,u_x + d(t)\,u = 0, \end{aligned} \tag{9}$$

with the arbitrary function $c_0(t)$, but $a(t)$, $b(t)$, $c_1(t)$, and $d(t)$ satisfying constraint (7a). One notices that Eq. (9) reduces to Eq. (2) when $a(t) = 6\,K_0(t)$, $b(t) = -K_0(t)$, $c_0(t) = -4\,K_1(t)$, $c_1(t) = h(t)$, and $d(t) = h(t)$, as well as constraint (7a) being satisfied automatically at the same time.

### B. Lax pair

Reference [13] mentions that the unique analytic solutions are supported by the PDE when such equation is Painlevé integrable, while there exist a Lax pair and $N$-soliton solution for the completely integrable PDE. In the present work, we will show that the complete integrability of Eq. (9) under constraint (7a) can be further confirmed by the existence of the Lax pair with time-dependent nonisospectral flow $\lambda'(t) = -d(t)\,\lambda(t)$, where $\lambda(t)$ is the nonisospectral eigenvalue. By virtue of the AKNS system, we consider the following linear eigenvalue problems for Eq. (9):

$$\Psi_x = U\,\Psi, \quad \Psi_t = V\,\Psi, \tag{10}$$

where $\Psi = (\psi_1, \psi_2)^T$ with $T$ representing the transpose of the vector, while $U$ and $V$ are taken the forms as

$$U = \begin{pmatrix} \lambda(t) & i\,u(x,t) \\ i\,u(x,t) & -\lambda(t) \end{pmatrix}, \quad V = \begin{pmatrix} A(x,t) & B(x,t) \\ C(x,t) & -A(x,t) \end{pmatrix}. \tag{11}$$

Meanwhile, the $2 \times 2$ matrices $U$ and $V$ should satisfy the zero curve equation,

$$U_t - V_x + [U,V] = 0, \tag{12}$$

by which the unknown functions in matrix $V$ can be determined as follows:

$$A(x,t) = -4\,b(t)\,\lambda(t)^3 - [x\,d(t) + 2\,b(t)\,u^2 + c_0(t)]\,\lambda(t), \tag{13a}$$

$$\begin{aligned} B(x,t) = &-4\,i\,b(t)\,u\,\lambda(t)^2 - 2\,i\,b(t)\,u_x\,\lambda(t) \\ &- i\,[x\,d(t)\,u + c_0(t)\,u + b(t)\,(2\,u^3 + u_{xx})], \end{aligned} \tag{13b}$$

$$\begin{aligned} C(x,t) = &-4\,i\,b(t)\,u\,\lambda(t)^2 + 2\,i\,b(t)\,u_x\,\lambda(t) \\ &- i\,[x\,d(t)\,u + c_0(t)\,u + b(t)\,(2\,u^3 + u_{xx})], \end{aligned} \tag{13c}$$

with the nonisospectral flow $\lambda'(t) = -d(t)\,\lambda(t)$ and constraints

$$a(t) = 6\,b(t), \quad c_1(t) = d(t). \tag{14}$$

It is straightforward to prove that the zero curve Eq. (12) with the determined matrices $U$ and $V$ gives rise to the completely integrable Eq. (9) under Constraint (14) and the nonisospectral eigenvalue $\lambda(t)$. Meanwhile, we note that Eq. (9) is completely integrable only if Constraint (14) is satisfied and such Lax constraints are one group of the special solutions for constraint (7a) which is derived from the Painlevé test. In such a case, we conclude that the Lax constraints of the complete integrability are more rigid than the Painlevé ones of the Painlevé integrability for Eq. (9).

## III. SOLITON SOLUTIONS AND SOLITON MANAGEMENT

In this section, before investigating the soliton dynamics and management for Eq. (9), we first pay attention to the explicit multisoliton solutions of Eq. (9) under Constraint (14) by virtue of the Hirota bilinear method [26]. Such a method has been effectively used to investigate the soliton, breather, and doubly periodic wave solutions to types of NLEEs [7,30].

In order to construct the analytic multisoliton solutions of Eq. (9) under Constraint (14), we apply a dependent variable transformation $u = -i\,[\ln(G/F)]_x$ with the complex conjugate functions $F(x,t)$ and $G(x,t)$ [30], and decouple Eq. (9) into a couple of bilinear equations under Constraint (14) as

$$\left[D_t + b(t)\,D_x^3 + c_0(t)\,D_x + x\,c_1(t)\,D_x\right](G \cdot F) = 0, \tag{15a}$$

$$D_x^2(G \cdot F) = 0, \tag{15b}$$

where the Hirota's bilinear operators $D_x$ and $D_t$ are defined by [26]

$$\begin{aligned} D_x^n D_t^m a \cdot b = &\left(\frac{\partial}{\partial x} - \frac{\partial}{\partial x'}\right)^n \left(\frac{\partial}{\partial t} - \frac{\partial}{\partial t'}\right)^m \\ &\times a(x,t) b(x',t')|_{x=x',t=t'}. \end{aligned} \tag{16}$$

For conveniently constructing soliton solutions for Eq. (9), with the same constraints (14), Eq. (9) can be rewritten as the following bilinear equations,

$$\left[D_t + b(t)\,D_x^3 + c_0(t)\,D_x + x\,c_1(t)\,D_x\right](g \cdot f) = 0, \tag{17a}$$

$$D_x^2(f \cdot f + g \cdot g) = 0, \tag{17b}$$

where $f$ and $g$ are real functions and assumed as follows [30]:

$$F = f - i\,g, \quad G = f + i\,g. \tag{18}$$

Under such an assumption, the variable transformation turns out to be

$$u = \left[2\,\arctan\left(\frac{g}{f}\right)\right]_x. \tag{19}$$

In the following section, based on Eq. (17) and Transformation (19), we will construct the multisoliton solutions for Eq. (9). In order to analytically discuss the soliton management through controlling the amplitudes and velocities of the soliton, we expand $g$ and $f$ into a power series of a small parameter $\epsilon$ as [7]

$$g = 1 + g_1\,\epsilon + g_2\,\epsilon^2 + g_3\,\epsilon^3 + \cdots, \tag{20a}$$

$$f = 1 + f_1\,\epsilon + f_2\,\epsilon^2 + f_3\,\epsilon^3 + \cdots. \tag{20b}$$

Substituting expression (20) into Eq. (17), via collecting coefficients of the same power of $\epsilon$, the analytic multisoliton solution for Eq. (9) can be constructed under some reasonable assumptions.

### A. One-soliton solution

In this part, to present the analytic expression of the one-soliton solution for Eq. (9), we assume that

$$g_1 = \exp(\theta_1), \quad f_1 = m_1\,\exp(\theta_1), \tag{21}$$

with $\theta_1 = n_1(t)\,x + \omega_1(t) + \eta_1$. Substituting the above expressions into Eq. (17), the unknown variables can be determined as

$$\begin{aligned} &m_1 = -1, \quad n_1(t) = \mu_1\,\exp\left[-\int c_1(t)\,dt\right], \\ &\omega_1(t) = -\int c_0(t)\,n_1(t)\,dt - \int b(t)\,n_1(t)^3\,dt, \end{aligned} \tag{22}$$

with the arbitrary constants $\eta_1$ and $\mu_1$. Therefore, the explicit analytic one-soliton solution can be expressed as

$$\begin{aligned} u &= \left[2\,\arctan\left(\frac{g}{f}\right)\right]_x = \left[2\,\arctan\left(\frac{1+g_1}{1+f_1}\right)\right]_x \\ &= n_1(t)\,\mathrm{sech}[n_1(t)\,x + \omega_1(t) + \eta_1]. \end{aligned} \tag{23}$$

Meanwhile, the amplitude $A$ and velocity $v$ for each soliton of Eq. (9) can be, respectively, derived as

$$A = |n_1(t)| = |\mu_1|\,\exp\left[-\int c_1(t)\,dt\right], \tag{24a}$$

$$v = c_0(t) + b(t)\,n_1(t)^2 - \frac{c_1(t)\,[\omega_1(t) + \eta_1]}{n_1(t)}. \tag{24b}$$

From Expression (24), it is obvious that the soliton amplitude is governed by the nonuniformity coefficient $c_1(t)$ and arbitrary constant $\mu_1$, while the velocity relies on the variable coefficients $d(t)$, $c_0(t)$, $c_1(t)$ and arbitrary constants $\eta_1$, $\mu_1$. To accomplish the purpose of soliton management for Eq. (9), we will emphasize how to control the soliton amplitude and velocity by changing the nonuniformity coefficient $c_1(t)$ and arbitrary constant $\mu_1$.

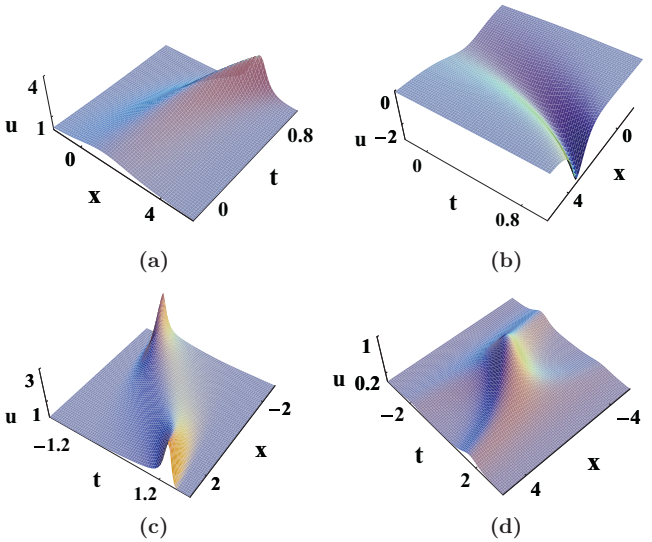


FIG. 1. (Color online) Evolution of the one-soliton via solution (23) for Eq. (9) under Constraint (14) when (a) $a(t) = 6, b(t) = 1, c_0(t) = 1, c_1(t) = -1, d(t) = -1, \mu_1 = 1, \eta_1 = 0$; (b) $a(t) = 6, b(t) = 1, c_0(t) = 1, c_1(t) = -1, d(t) = -1, \mu_1 = -1, \eta_1 = 0$; (c) $a(t) = 6, b(t) = 1, c_0(t) = 1, c_1(t) = -t, d(t) = -t, \mu_1 = 1, \eta_1 = 0$; (d) $a(t) = 6, b(t) = 1, c_0(t) = 0, c_1(t) = t, d(t) = t, \mu_1 = 1, \eta_1 = 0$.

Firstly, our interest will be devoted to the effect of the arbitrary constant $\mu_1$ when the nonuniformity coefficient $c_1(t)$ is invariant. Via Expression (23), we find that there exist two families of solitons, namely, elevation and depression solitons, which depend on the sign of $\mu_1$. Generally speaking, for $\mu_1 > 0$, the elevation soliton is derived for Eq. (9), while the depression soliton appears in the case of $\mu_1 < 0$. Furthermore, the soliton amplitude and speed (velocity in magnitude) gradually increase with the increase of $|\mu_1|$.

In the following part, we will construct different types of one-soliton profiles depending on the nonuniformity coefficient $c_1(t)$ under Constraint (14). We assume that $c_1(t)$ does not vary with time [i.e., $c_1(t)$ is a constant]. When $c_1(t) > 0$, the amplitude of the one soliton decreases with time and correspondingly the soliton width broadens with time. On the contrary, when $c_1(t) < 0$, the one-soliton amplitude increases gradually and the soliton width gradually decreases as a result. Figure 1(a) presents the evolution of the elevation soliton with $\mu_1 = 1$ and $c_1(t) = -1$, from which one can observe that the soliton amplitude monotonously grows with the decreasing of the soliton width due to the presence of the negative $c_1(t)$. Such variation is consistent with the analytical expression of the soliton amplitude $A = \exp(t)$, which exponentially increases with $t$. Correspondingly, the similar amplitude and width variation are identical to those for the depression soliton with $\mu_1 = -1$ and $c_1(t) = -1$, as shown in Fig. 1(b).

In Fig. 1(c), we describe the one-soliton dynamics when $c_1(t)$ is selected as the monotonous function decreasing with time and $\mu_1$ is supposed to be a positive constant [$c_1(t) = -t$, $\mu_1 = 1$]. To discuss the soliton management for Eq. (9) under Constraint (14), the corresponding amplitude for each soliton can be expressed as $A = \exp(t^2/2)$, from which we figure out that the soliton with minimal amplitude takes place at the moment of $t = 0$. Such a development trend can also

be observed in Fig. 1(c), that is, the soliton propagates with the amplitude attenuating but width broadening as the time gradually approaches to zero. If $c_1(t) = d(t) = t$, $c_0(t) = 0$ and other parameters are selected as same as those in Fig. 1(c), another different type of soliton can be derived in Fig. 1(d), in which the soliton amplitude and width variation are opposite to those in Fig. 1(c), that is, at the moment of $t = 0$, the soliton amplitude reaches to the maximal value but the soliton width is compressed into the narrowest one. In addition, the variation of the soliton amplitude in Fig. 1(d) accords with the analytical expression $A = \exp(-t^2/2)$. Furthermore, when the soliton in Fig. 1(d) is compared with the two-soliton bound state in Ref. [31], we notice that both of them can generate high-amplitude waves along the propagation direction. However, the mechanism for the formation of the high-amplitude waves is different. In Fig. 1(d), the formation of high-amplitude waves is caused by the soliton compression effect, while in Ref. [31], the generation of high-amplitude waves is induced by the two-soliton interaction in the bound state.

### B. Two solitons and breather

Based on the one-soliton solution for Eq. (9) under Constraint (14), we have studied the compression of the soliton by manipulating the nonuniformity coefficient $c_1(t)$. Generally speaking, the soliton interaction plays a role in determining the physical features of the dynamical systems and benefits the relevant applications in various fields [32]. Therefore, it is necessary to investigate the similar soliton management problems on the two-soliton interaction. The Hirota bilinear method can be employed to generate the multisoliton solutions [7]. For instance, the two-soliton solution can be constructed as

$$
\begin{aligned}
u &= \left\{ 2 \arctan\left[ \frac{1 + \exp(\theta_1) + \exp(\theta_2) + N_1 \exp(\theta_1 + \theta_2)}{1 + m_1 \exp(\theta_1) + m_2 \exp(\theta_2) + M_1 \exp(\theta_1 + \theta_2)} \right] \right\}_x, \\
\theta_i &= n_i(t)\, x + \omega_i(t) + \eta_i, n_i(t) = \mu_i \exp\left[ -\int c_1(t)\, dt \right], \quad (i = 1,2), \\
\omega_i(t) &= -\int c_0(t)\, n_i(t)\, dt - \int b(t)\, n_i(t)^3\, dt, \quad m_i = -1, \quad (i = 1,2), \\
N_1 &= M_1 = -\frac{(\mu_1 - \mu_2)^2}{(\mu_1 + \mu_2)^2},
\end{aligned}
\tag{25}
$$

where $\mu_i$ and $\eta_i$ $(i = 1,2)$ are arbitrary parameters. From the expression of the two-soliton solution, it is observed that the amplitude and velocity of each soliton in the two-soliton solution can also be influenced by $c_1(t)$. Thus, it is possible to form different types of two-soliton profiles if one manages to control the function $c_1(t)$.

Figure 2(a) describes the evolution of the two-soliton interaction with unequal amplitudes and velocities when the nonuniformity coefficient $c_1(t)$ is a negative constant. From Fig. 2(a), one observes that the soliton amplitudes increase but the soliton widths get compressed, which can also be interpreted by Fig. 2(b). Meanwhile, it is noted from Fig. 2(b) that the two solitons interact with each other without a phase shift, and then the two slide over each other. Furthermore, we present another two scenarios of interactions between the two neighboring solitons as shown in Fig. 3, in which $c_1(t)$ is taken as $-t$ in Fig. 3(a) and $t$ in Fig. 3(b), respectively. The results suggest that the main features of the two-soliton interaction have a similar appearance to those of the one-soliton case, that is, the soliton amplitudes and widths vary with time along the propagation directions, except for the different variation types due to the different choices of $c_1(t)$. In Fig. 3(a), the soliton amplitudes decrease to the minimal value but the soliton widths increase to the maximal value at the moment of $t = 0$. As a

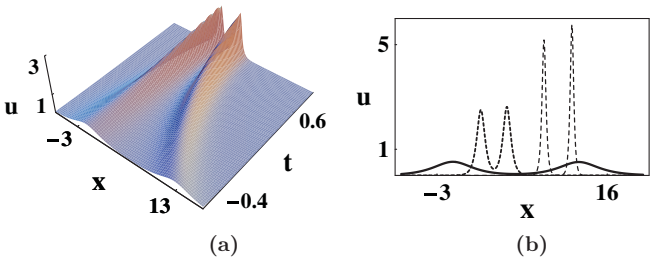


FIG. 2. (Color online) Interaction of the two solitons via solution (25) for Eq. (9) under Constraint (14) when (a) $a(t) = 6, b(t) = 1, c_0(t) = 0, c_1(t) = -1, d(t) = -1, \mu_1 = 1, \eta_1 = 0, \mu_2 = 0.9, \eta_2 = 0$. (b) Profiles of (a) when $t = -0.6$ (solid line), $t = 1$ (bold dashed line), and $t = 1.75$ (dashed line).

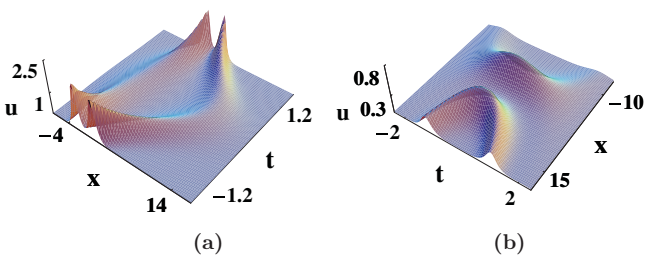


FIG. 3. (Color online) Interaction of the two solitons via solution (25) for Eq. (9) under Constraint (14) when $a(t) = 6, b(t) = 1, \mu_1 = 0.6, \eta_1 = 0, \mu_2 = 0.5, \eta_2 = 0$ with (a) $c_0(t) = 1, c_1(t) = -t, d(t) = -t$; (b) $c_0(t) = 0, c_1(t) = t, d(t) = t$.

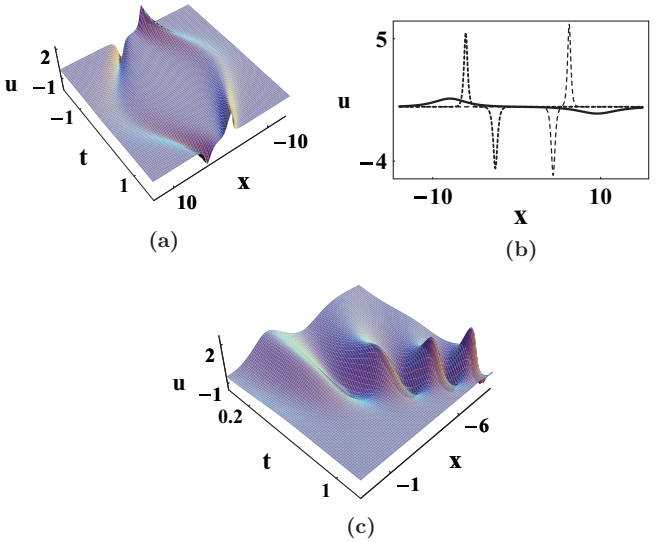


FIG. 4. (Color online) Interaction between an elevation soliton and a depression soliton via solution (25) for Eq. (9) under Constraint (14) when (a) $a(t) = 6$, $b(t) = 1$, $c_0(t) = 0$, $c_1(t) = -t$, $d(t) = -t$, $\mu_1 = 0.6$, $\eta_1 = 0$, $\mu_2 = -0.5$, $\eta_2 = 0$. (b) Profiles of (a) when $t = 0$ (solid line), $t = -2.1$ (bold dashed line), and $t = 2.15$ (dashed line). (c) Evolution of a breather via solution (26) for Eq. (9) under Constraint (14) when $a(t) = 6, b(t) = 1, c_0(t) = 0, c_1(t) = -1$, $d(t) = -1$, $p = 0.5$, $q = 1$.

comparison, the two solitons have the highest amplitudes but narrowest widths at the moment of $t = 0$ in Fig. 3(b).

Similarly, the interaction between the two depression solitons can be studied via supposing the two parameters $\mu_1$ and $\mu_2$ to be negative, and the interaction features for the depression solitons are similar to the elevation cases in Figs. 2 and 3, that is, the amplitudes and velocities for the depression solitons have the same development trend when the nonuniformity term coefficient $c_1(t)$ is chosen as the same function for the elevation case. For further description of the two-soliton interaction, it is necessary to discuss the interaction between an elevation and a depression, as shown in Figs. 4(a) and 4(b). Moreover, in the far field of the left side [corresponding to the bold dashed line in Fig. 4(b)], the elevation leaves behind the depression but the amplitude of the elevation is larger than that of the depression. As $T$ approaches zero, both the elevation and depression amplitudes decrease to the minimal values, but the soliton widths achieve the maximal values [solid line in Fig. 4(b)], which is due to the effect of the nonuniformity term $c_1(t)\,x$. With time evolution, the solitons are compressed into the ones with narrow widths again, and as a result the soliton amplitudes gradually increase in the far field of the right side [dashed line in Fig. 4(b)]. Meanwhile, the elevation soliton goes ahead of the depression one (i.e., the elevation and depression preserve their identities after the collision), except for the phase shifts.

Based on the two-soliton solution derived, we will construct the breather which is an isolated wave form with periodic pulsating or oscillating and has the energy concentrated in localized range [33]. Such a structure can be realized by assuming the two complex conjugate parameters as $\mu_1 = p + i\,q$ and $\mu_2 = p - i\,q$ ($p, q$ are real constants). Substituting the two complex conjugate parameters into Expression (25) for the two-soliton solution, we can obtain the explicit expression of the breather for Eq. (9) under Constraint (14) as follows:

$$
\begin{aligned}
u &= \left[2\,\arctan\left(\frac{g}{f}\right)\right]_x,\\
g &= \exp(-p\,\Upsilon) + \frac{q^2}{p^2}\,\exp(p\,\Upsilon) + 2\,\cos\Omega,\\
f &= \exp(-p\,\Upsilon) + \frac{q^2}{p^2}\,\exp(p\,\Upsilon) - 2\,\cos\Omega,\\
\Upsilon &= x\,\exp\left[-\int c_1(t)\,dt\right] - (p^2 - 3\,q^2)\int b(t)\\
&\quad\times \exp\left[-3\int c_1(t)\,dt\right]dt\\
&\quad-\int c_0(t)\,\exp\left[\int c_1(t)\,dt\right]dt,\\
\Omega &= q\,x\,\exp\left[-\int c_1(t)\,dt\right] + (q^3 - 3\,p^2\,q)\int b(t)\\
&\quad\times \exp\left[-3\int c_1(t)\,dt\right]dt\\
&\quad-q\int c_0(t)\,\exp\left[\int c_1(t)\,dt\right]dt.
\end{aligned}
\tag{26}
$$

With the suitable choice of the variable coefficients and parameters, we depict the evolution of breather in Fig. 4(c), from which we observe that the breather amplitude gradually increases and as a result the breather is gradually compressed due to the presence of the nonuniformity term $c_1(t)\,x$. Similar to the two-soliton interaction, we can construct another type of breather by the different choices of $c_1(t)$, which plays a crucial role in the soliton and breather dynamics.

### C. Three-soliton solution and interaction between a breather and a soliton

According to the above procedure of deriving the one- and two-soliton solutions by virtue of the Hirota bilinear method, the three-soliton solution for Eq. (9) under Constraint (14) can be constructed as follows:

$$
\begin{aligned}
u &= \left[2\,\arctan\left(\frac{1+g_1+g_2+g_3}{1+f_1+f_2+f_3}\right)\right]_x,\\
g_1 &= \exp(\theta_1) + \exp(\theta_2) + \exp(\theta_3),\\
f_1 &= m_1\,\exp(\theta_1) + m_2\,\exp(\theta_2) + m_3\,\exp(\theta_3),\\
g_2 &= N_{12}\,\exp(\theta_1+\theta_2) + N_{23}\,\exp(\theta_2+\theta_3)\\
&\quad + N_{13}\,\exp(\theta_1+\theta_3),\\
f_2 &= M_{12}\,\exp(\theta_1+\theta_2) + M_{23}\,\exp(\theta_2+\theta_3)\\
&\quad + M_{13}\,\exp(\theta_1+\theta_3),\\
g_3 &= N_{123}\,\exp(\theta_1+\theta_2+\theta_3),\\
f_3 &= M_{123}\,\exp(\theta_1+\theta_2+\theta_3),\\
\theta_i &= n_i(t)\,x + \omega_i(t) + \eta_i,\\
n_i(t) &= \mu_i\,\exp\left[-\int c_1(t)\,dt\right],\quad (i = 1,2,3),\\
\omega_i(t) &= -\int c_0(t)\,n_i(t)\,dt - \int b(t)\,n_i(t)^3\,dt,
\end{aligned}
$$

$$m_i = -1, \quad (i = 1,2,3),$$
$$M_{ij} = N_{ij} = -\frac{(\mu_i - \mu_j)^2}{(\mu_i + \mu_j)^2}, \quad (i,j = 1,2,3, \quad i < j),$$
$$M_{123} = -N_{123} = \frac{(\mu_1 - \mu_2)^2 (\mu_2 - \mu_3)^2 (\mu_1 - \mu_3)^2}{(\mu_1 + \mu_2)^2 (\mu_2 + \mu_3)^2 (\mu_1 + \mu_3)^2}, \tag{27}$$

where $\mu_i$'s and $\eta_i$'s $(i = 1,2,3)$ are the arbitrary parameters. Similar to the two-soliton solution, it is possible to form different types of three-soliton interactions if one manages to control the function $c_1(t)$. Moreover, the soliton amplitude and velocity variation in the three-elevation and three-depression interactions are similar to the corresponding two-soliton interactions when $c_1(t)$ is chosen as the identical function.

Therefore, we will pay attention to the interaction between the elevation and depression, as shown in Fig. 5. Figure 5(a) depicts the interaction between two elevations and a depression, from which we observe that the compression phenomenon also occurs in such a case. Furthermore, the depression leaves behind the elevations but the depression amplitude is larger than those of the elevations in the far field of the left side [corresponding to the solid line in Fig. 5(b)]. As $T$ approaches zero, the depression collides with the left elevation and then overtakes it. Meanwhile, the elevation and depression amplitudes gradually attenuate to the minimal values, but the soliton widths gradually increase to the maximal values [bold dashed line in Fig. 5(b)], which is due to the effect of the nonuniformity term $c_1(t)\,x$. In the far field of the right side, the depression goes ahead of the two elevations, and the two elevations have changed their positions. At the same time,

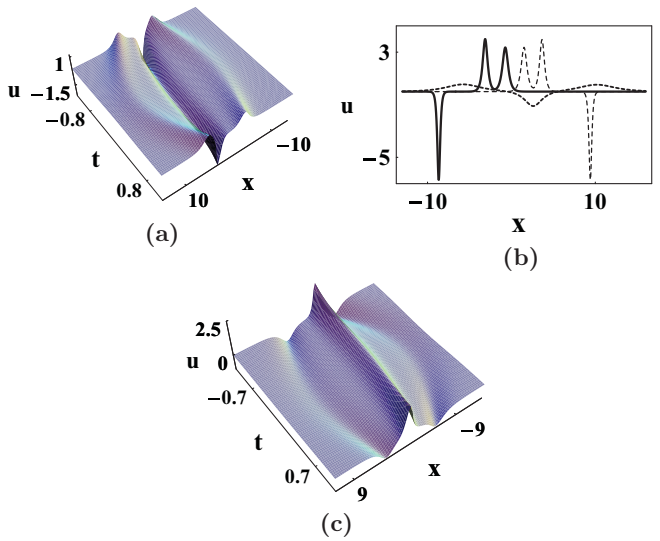


FIG. 5. (Color online) Interaction between two elevation solitons and a depression soliton via solution (27) for Eq. (9) under Constraint (14) when (a) $a(t) = 6$, $b(t) = 1$, $c_0(t) = 0$, $c_1(t) = -t$, $d(t) = -t$, $\mu_1 = -1$, $\mu_2 = 0.5$, $\mu_3 = 0.6$, $\eta_1 = 0$, $\eta_2 = 0$, $\eta_3 = 0$. (b) Profiles of (a) when $t = -1.95$ (solid line), $t = 0$ (bold dashed line), and $t = 1.95$ (dashed line). (c) Interaction between an elevation and two depressions via solution (27) for Eq. (9) under Constraint (14) when $a(t) = 6$, $b(t) = 1$, $c_0(t) = 0$, $c_1(t) = -t$, $d(t) = -t$, $\mu_1 = 1$, $\mu_2 = -0.5$, $\mu_3 = -0.6$, $\eta_1 = 0$, $\eta_2 = 0$, $\eta_3 = 0$.

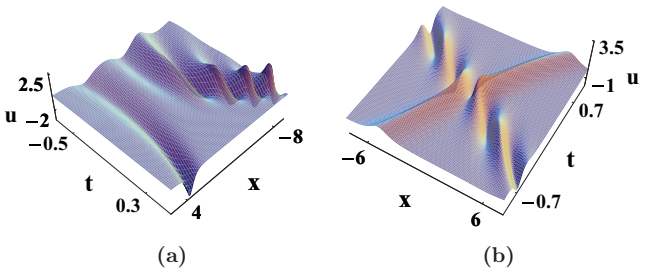


FIG. 6. (Color online) Interaction between a breather and a soliton via solution (27) for Eq. (9) under Constraint (14) when $a(t) = 6$, $b(t) = 1$, $c_0(t) = 0$, $\mu_2 = 1 + 2i$, $\mu_3 = 1 - 2i$, $\eta_1 = 0$, $\eta_2 = 0$, $\eta_3 = 0$ with (a) $\mu_1 = -1.75$, $c_1(t) = -1$, $d(t) = -1$; (b) $\mu_1 = 2$, $c_1(t) = t$, $d(t) = t$.

the soliton amplitudes gradually increase, and as a result the soliton widths are compressed again [dashed line in Fig. 5(b)]. Correspondingly, the interaction between an elevation and two depressions is shown in Fig. 5(c), in which the interaction process and compression phenomenon are similar to those in Figs. 5(a) and 5(b).

Similar to the technique employed in Ref. [30], the interaction between a breather and a soliton can be derived from the three-soliton solution by supposing the three arbitrary parameters as $\mu_1 = p + i\,q$, $\mu_2 = p - i\,q$, and $\mu_3$ ($p$, $q$, $\mu_3$ are real constants). Due to the complicated expression for describing such interaction, we just present the graphic illustrations in Fig. 6 by symbolic computation [28,29]. Figure 6(a) describes the interaction between a depression and a breather, from which we observe that the depression moves toward the breather when $t < 0$ but the trajectories of the two are dictated as $t > 0$. During the propagation of the depression and breather, both of them are compressed and correspondingly their amplitudes gradually increase with time evolution. Moreover, the interaction between the elevation and breather is shown in Fig. 6(b), in which the elevation and breather are gradually compressed and the amplitudes monotonously increase as $t$ approaches zero, but after such a moment the amplitudes attenuate and the widths increase gradually along the propagation directions.

## IV. NUMERICAL SIMULATION OF SOLITON DYNAMICS

In this section, the finite difference method will be employed to simulate dynamics of the typical one soliton for Eq. (9) with the following conditions: (i) Constraint (14) is completely fulfilled; (ii) Constraint (14) is finitely perturbed. As we know, Eq. (9) has the standard mKdV equation as its special case, which supports the soliton solutions with balance between the nonlinearity and dispersion [$a(t) = 6b(t)$ and $c_0(t) = c_1(t) = d(t) = 0$ in Eq. (9)]. In general, we connect Eq. (9) to the unsteady (time-dependent) physical system describing the solitary waves with the second-order nonlinearity and first-order dispersion in the weakly nonlinear theory [34]. In such a case, coefficients of the first-order nonlinearity approach zero, while $a(t)$, $b(t)$, and $d(t)$ are related to the time-dependent second-order nonlinearity coefficient, dispersion coefficient, and shoaling coefficient. Specifically,

the linear phase velocity $xc_1(t)+c_0(t)$ is not only time dependent, but also linear with the spatial coordinate, which can be explained with the varying topography in the physical system.

Thus, the generation of solitons under Constraint (14) can be explained by two types of balances in the physical system: (i) balance between the first-order dispersion and second-order nonlinearity; (ii) balance between the linear phase velocity and shoaling effect. Our analytical soliton solutions are constructed with both balances. However, it may be less appropriate to use the analytical solutions to describe the type of system in Eq. (9) if those balances are not completely achieved. For such a condition, Eq. (9) is solved numerically with a finite difference form:

$$\frac{u_j^{n+1}-u_j^{n-1}}{\Delta t}+a(t^n)\left(u_j^n\right)^2\frac{u_{j+1}^n-u_{j-1}^n}{\Delta x}+b(t^n)\frac{u_{j+2}^n-2u_{j+1}^n+2u_{j-1}^n-u_{j-2}^n}{\Delta x^3}+[c_0(t^n)+x_jc_1(t^n)]\frac{u_{j+1}^n-u_{j-1}^n}{\Delta x}+2d(t^n)u_j^n=0. \quad (28)$$

For the first step, $(u_j^{n+1}-u_j^{n-1})/(2\Delta t)$ is replaced by $(u_j^1-u_j^0)/\Delta t$, where $u_j^0$ is the initial value. We assume that the reasonably large spatial domain is chosen with the lateral boundary conditions $u(-L,t)=u(L,t)=0$, where $-L$ and $L$ are the two edges of the domain. Such a numerical scheme has been used and developed for the KdV-type equation [35]. In our simulation, we employ the one-soliton solution (23) with the parameters in Fig. 1(a) as the initial conditions, and properly choose $(\Delta x,\Delta t)=(5\times10^{-2},2\times10^{-5})$.

In Fig. 7(a), we demonstrate good agreement between the soliton profiles at $t=1$ with the analytical and numerical approaches under Constraint (14). As mentioned, such a case is based on the balance between the dispersion and nonlinearity, as well as the balance between the linear phase velocity and shoaling effect. Here, $\pm20\%$ perturbation on $a(t)=6b(t)$ in Constraint (14) is first considered, and the simulation results are illustrated in Fig. 7(b). It can be observed that small oscillating tails are separated backward from the soliton for both unbalanced cases. However, with the stronger nonlinearity $[a(t)=7.2b(t)]$, the soliton gets compressed to hold a larger amplitude than that for the balanced case $[a(t)=6b(t)]$ at $t=1$, and appears to acquire an increased velocity during propagation. As a comparison, the situation with the stronger dispersion $[a(t)=4.8b(t)]$ is fundamentally opposite. In fact, perturbation on $a(t)=6b(t)$ in Constraint (14) may decide whether the nonlinear focusing or dispersion effect dominates on the soliton dynamics. Following a similar procedure, we propose $\pm20\%$ perturbation on $c_1(t)=d(t)$ in Constraint (14), and simulate the soliton dynamics, as seen in Fig. 7(c). We find that with the larger absolute value of $c_1(t)$ $[c_1(t)=1.2d(t)]$, the soliton amplitude at $t=1$ cannot reach the one with the balance of $c_1(t)=d(t)$, and the soliton velocity decreases correspondingly. When the absolute value of $d(t)$ is larger $[c_1(t)=0.8d(t)]$, the soliton propagates faster than that with $c_1(t)=d(t)$, and its amplitude exceeds the one in the balanced case.

Therefore, generation of solitons in the system governed by Eq. (9) with Constraint (14) fulfilled is based on two types of balances mentioned above. The soliton dynamics is more complicated if such a constraint is not satisfied, as investigated

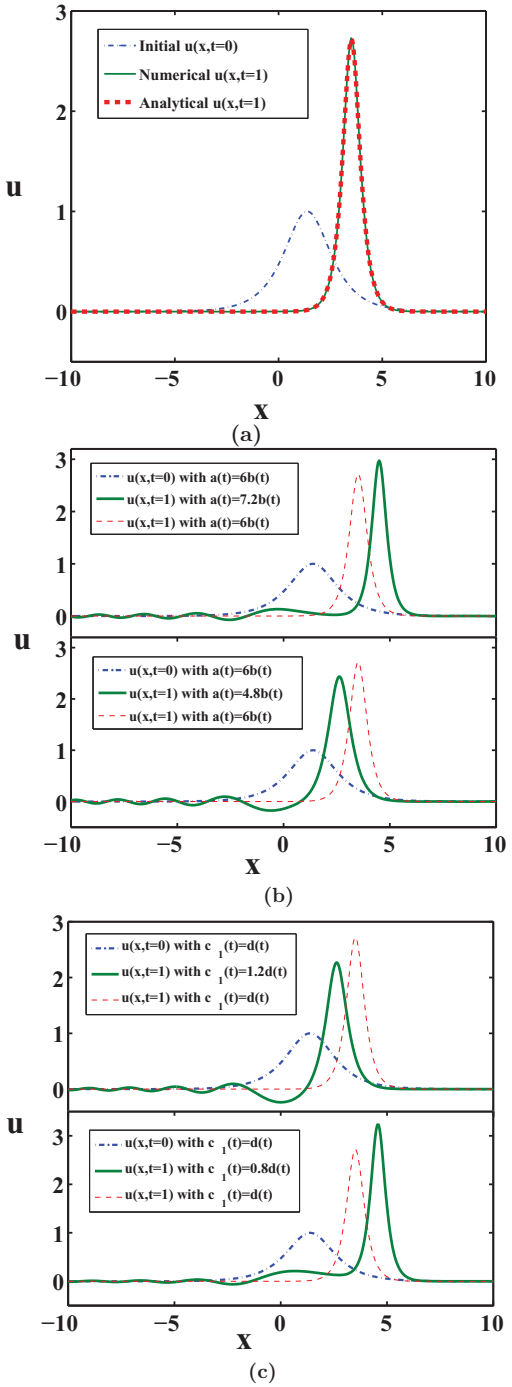


FIG. 7. (Color online) Initial condition $u(x,t=0)$ is chosen as the one-soliton solution (23) with the parameters in Fig. 1(a). (a) Comparison of the soliton profiles $u(x,t=1)$ between the analytical and numerical approaches with Constraint (14) completely satisfied. (b) Comparison between the soliton profiles with $a(t)=6b(t)$ completely satisfied and with $a(t)=6b(t)$ $\pm20\%$ perturbed $[a(t)=7.2b(t)=7.2$ in the upper panel and $a(t)=4.8b(t)=4.8$ in the lower panel]. (c) Comparison between the soliton profiles with $c_1(t)=d(t)$ completely satisfied and with $c_1(t)=d(t)$ $\pm20\%$ perturbed $[c_1(t)=1.2d(t)=-1.2$ in the upper panel and $c_1(t)=0.8d(t)=-0.8$ in the lower panel].

in our numerical simulation. In fact, we have proposed the elevation solitons in Fig. 7, and the depression ones can be addressed in a similar manner.

## V. CONCLUSIONS

In this paper, we have analyzed the integrability of the variable-coefficient mKdV equation (1) which might possess applications in the interfacial waves in two-layer liquid and Alfvén waves in a collisionless plasma. Under constraint (7a), we have found generalized integrable form (9) of Eq. (1) in the sense of Painlevé integrability. Moreover, Lax pair (11) with time-dependent nonisospectral flow of Eq. (9) has been established under the Lax constraint (14) which seems to be more rigid than the Painlevé constraint (7a). To discuss the soliton management, the soliton solutions for Eq. (9) under Constraint (14) have been constructed by the Hirota bilinear method, and then the one-soliton (23), two-soliton (25), and three-soliton (27) solutions have been presented.

As the basic parameters of the dynamics of a soliton, the amplitude (or width) and frequency (or velocity) have been applied to show the main features of the soliton. Results have revealed that we can achieve the purpose of soliton management by controlling the nonuniformity coefficient $c_1(t)$ and constant $\mu_i$. The conclusions inferred from the above discussions can be presented as follows:

(1) As seen in Fig. 1, Eq. (9) supports two families of solitons (elevation and depression) depending on the sign of $\mu_i$, which can also affect the soliton amplitude and velocity.

(2) Different types of one-soliton profiles and soliton interactions with unequal amplitudes and velocities can be formed when $c_1(t)$ is chosen to be different functions, which have been described in Figs. 1–3.

(3) As seen in Figs. 1(a) and 1(b), when $c_1(t)$ is a negative (positive) constant, the amplitude of each soliton monotonously increases (decreases) with time and correspondingly the soliton is compressed (broadened) with time.

(4) When $c_1(t)$ is supposed to be the linear function of $t$ in Figs. 1(c) and 1(d), each soliton is gradually compressed (broadened) and as a result the soliton amplitude gradually increases (decreases) to the maximal (minimal) value at the moment of $t = 0$. While after such moment each soliton amplitude begins to decrease (increase) and corresponding the width of soliton is broadened (compressed) along the propagation direction.

Moreover, the above conclusions are also consistent with the features for the dynamics of the breather in Fig. 4(c), as well as the interaction between a breather and a soliton in Fig. 6. Besides the analytic procedure, numerical simulation has been proposed to illustrate the soliton dynamics with Constraint (14) finitely perturbed, as seen in Figs. 7(b) and 7(c). The results have inferred that the soliton amplitude and velocity are influenced when the balances in Constraint (14) are perturbed, and oscillating wave tails are observed to separate backward from the soliton in such a situation.

## ACKNOWLEDGMENTS

We express our sincere thanks to the referees for their valuable suggestions. We are also very grateful to all the members of our discussion group for their beneficial comments. This work has been supported by the National Natural Science Foundation of China under Grant No. 60772023, by the Open Fund (Grant No. BUAA-SKLSDE-09KF-04) and Supported Project (Grant No. SKLSDE-2010ZX-07) of the State Key Laboratory of Software Development Environment, Beijing University of Aeronautics and Astronautics, by the National Basic Research Program of China (973 Program) under Grant No. 2005CB321901, by the Specialized Research Fund for the Doctoral Program of Higher Education (Grants No. 20060006024 and No. 200800130006), Chinese Ministry of Education, and by the Doctoral Innovation Foundation (Grants No. 30-0350 and No. 30-0366), Beijing University of Aeronautics and Astronautics.

[1] N. J. Zabusky and M. D. Kruskal, Phys. Rev. Lett. **15**, 240 (1965).
[2] M. J. Ablowitz and P. A. Clarkson, *Solitons, Nonlinear Evolution Equations and Inverse Scattering* (Cambridge University Press, Cambridge, 1991).
[3] B. A. Malomed, *Soliton Management in Periodic Systems* (Springer, New York, 2006).
[4] K. Porsezian, A. Hasegawa, V. N. Serkin, T. L. Belyaeva, and P. Ganapathy, Phys. Lett. A **361**, 504 (2007).
[5] P. G. Kevrekidis, G. Theocharis, D. J. Frantzeskakis, and B. A. Malomed, Phys. Rev. Lett. **90**, 230401 (2003).
[6] S. Clarke, B. A. Malomed, and R. Grimshaw, Chaos **12**, 8 (2002).
[7] C. C. Mak, K. W. Chow, and K. Nakkeeran, J. Phys. Soc. Jpn. **74**, 1449 (2005).
[8] R. Ganapathy, K. Porsezian, and A. Hasegawa, IEEE J. Quantum Electron. **44**, 383 (2008); K. Porsezian, R. Ganapathy, and A. Hasegawa, *ibid.* **45**, 1577 (2009).
[9] K. R. Helfrich, W. K. Melville, and J. W. Miles, J. Fluid Mech. **149**, 305 (1984).
[10] H. H. Chen and C. S. Liu, Phys. Rev. Lett. **37**, 693 (1976).
[11] F. Calogero and A. Degasperis, Lett. Nuovo Cimento **16**, 425 (1976).
[12] V. N. Serkin, A. Hasegawa, and T. L. Belyaeva, Phys. Rev. Lett. **98**, 074102 (2007).
[13] A. Kundu, Phys. Rev. E **79**, 015601 (2009).
[14] A. V. Slyunyaev, J. Exp. Theor. Phys. **92**, 529 (2001).
[15] T. I. Karpman and H. Ono, J. Phys. Soc. Jpn. **34**, 1073 (1973).
[16] S. Y. Lou and H. Y. Ruan, Acta Phys. Sin. **41**, 182 (1992), in Chinese.
[17] W. L. Chan and K. S. Li, J. Phys. A **27**, 883 (1994).
[18] W. L. Chan and X. Zhang, J. Phys. A **28**, 407 (1995).
[19] Z. Y. Yan, Commun. Nonlin. Sci. Numer. Simulat. **4**, 284 (1999).
[20] C. Q. Dai, J. M. Zhu, and J. F. Zhang, Chaos Soliton Fract. **27**, 881 (2006).
[21] S. Zhang and T. C. Xia, Phys. Lett. A **372**, 1741 (2008).

[22] Q. Feng, Y. T. Gao, X. H. Meng, X. Yu, Z. Y. Sun, T. Xu, and B. Tian, Int. J. Mod. Phys. B **25**, 723 (2011).
[23] J. Weiss, M. Tabor, and G. Carnevale, J. Math. Phys. **24**, 522 (1983).
[24] M. Jimbo, M. D. Kruskal, and T. Miwa, Phys. Lett. A **92**, 59 (1982).
[25] M. J. Ablowitz, D. J. Kaup, A. C. Newell, and H. Segur, Phys. Rev. Lett. **31**, 125 (1973).
[26] R. Hirota, *The Direct Method in Soliton Theory* (Cambridge University Press, Cambridge, 2004).
[27] X. G. He, D. Zhao, L. Li, and H. G. Luo, Phys. Rev. E **79**, 056610 (2009).
[28] M. P. Barnett, J. F. Capitani, J. Von Zur Gathen, and J. Gerhard, Int. J. Quantum Chem. **100**, 80 (2004); B. Tian and Y. T. Gao, Phys. Lett. A **362**, 283 (2007); X. Yu, Y. T. Gao, Z. Y. Sun, and Y. Liu, Phys. Rev. E **83**, 056601 (2011).
[29] G. Das and J. Sarma, Phys. Plasmas **6**, 4394 (1999); Y. T. Gao and B. Tian, Europhys. Lett. **77**, 15001 (2007); Y. Liu, Y. T. Gao, T. Xu, X. Lü, Z. Y. Sun, X. H. Meng, X. Yu, and X. L. Gai, Z. Naturforsch. A **65**, 291 (2010).
[30] K. W. Chow, Wave Motion **35**, 71 (2002); K. W. Chow, R. H. Grimshaw, and E. Ding, *ibid.* **43**, 158 (2005); Z. Y. Sun, Y. T. Gao, X. Yu, X. H. Meng, and Y. Liu, *ibid.* **46**, 511 (2009).
[31] R. Atre, P. K. Panigrahi, and G. S. Agarwal, Phys. Rev. E **73**, 056611 (2006).
[32] M. Karlsson, D. J. Kaup, and B. A. Malomed, Phys. Rev. E **54**, 5802 (1996).
[33] K. G. Lamb, O. Polukhina, T. Talipova, E. Pelinovsky, W. Xiao, and A. Kurkin, Phys. Rev. E **75**, 046306 (2007); Z. Y. Sun, Y. T. Gao, X. Yu, W. J. Liu, and Y. Liu, *ibid.* **80**, 066608 (2009); Z. Y. Sun, Y. T. Gao, X. Yu, and Y. Liu, Europhys. Lett. **93**, 40004 (2011).
[34] R. J. Small and R. P. Hornby, Ocean Model. **8**, 395 (2005).
[35] P. E. Holloway, E. Pelinovsky, T. Talipova, and B. Barnes, J. Phys. Oceanogr. **27**, 871 (1997).